Distributed Relaxation Processes in Sensory Adaptation

Spatial nonuniformity in receptors can explain both the curious dynamics and logarithmic statics of adaptation.

John Thorson and Marguerite Biederman-Thorson

One strategy of physiologists is based upon the fact that the measured dynamics of a process can sometimes offer guidance in the search for underlying mechanism. Although this approach—called "transfer-function analysis" or "input-output analysis"—has often proved helpful, it has not led to notable insight when applied to single cells of receptor organs. Our purpose in this article is to describe this apparent paradox, and to suggest one resolution of it.

The property of receptor cells that causes this difficulty is best introduced within the context of the usual starting procedure of such an analysis, as applied to any system. First, one imposes small steplike or sinusoidal changes upon an input and measures the resulting fluctuations in time of an output. Often these fluctuations can be described in a compact mathematical form; comparison with the known equations of familiar physical processes (diffusion, transport delays, chemical reactions, or other likely phenomena) may then suggest hypotheses about the events underlying the system studied. If these hypotheses can be tested, the study is at least begun.

This procedure works best if the dynamic description turns out to involve linear differential equations, for if the system is fundamentally nonlinear special problems arise at every stage. In fact, many physiological processes do exhibit nearly linear dynamics if the input changes are made sufficiently small; a few examples not directly involving receptors will illustrate the kind of insight obtainable if the strategy succeeds. Lateral inhibition in the *Limulus* visual system cannot follow changes in presynaptic nerve-impulse rate if the changes occur too rapidly; this dynamic effect is commensurate with—and may well be determined by—the nearly exponential time courses of individual inhibitory synaptic potentials (*1*). In another example, the way in which an insect responds to visual patterns moved at various velocities suggests underlying circuitry and time delays, the neural equivalents of which are now being sought (*2–5*). In still another, the dynamic relationship between length and tension in striated muscle suggests the testable hypothesis that it reflects fluctuations in the number and configurations of cross-bridges linking actin and myosin filaments (*6*).

In cases such as these, the above strategy has been effective because the nearly linear dynamics measured have been describable by ordinary first- or second-order differential equations and thus have had discernible implications at the next lower levels of explanation. Indeed, one might form the impression that linearity guarantees a measure of success.

It is here that the difficulty associated with sensory transduction arises. Although most receptor cells do respond nearly linearly to small perturbations of their inputs, their characteristic dynamics have not generally served to suggest testable ideas about their physical nature. The most common problem is that the time courses of the measured responses to step inputs often obey closely a power law, changing as t^{-k} (where t is time and k is a constant between 0 and 1) over several decades of time after the stimulus; moreover, the frequency response can involve the kth power of frequency, and the corresponding linear differential equations, as we shall see, can be of *fractional order*. Thus the usual exponential decays and integral-order differential equations—the ordinary guides to likely physical explanations—are not explicitly available.

To try to relate these linear power-law dynamics to cellular physiology, we have borrowed some of the "distributed-relaxation" methods from the fields of electrophysics and polymer viscoelasticity. Surprisingly, the explanations to which we have been led not only interpret the power-law dynamics for small input changes, but also offer a novel basis for the steady-state nonlinear "range compression" observed when the inputs to such transducers undergo large changes.

The linear power-law dynamics should not be confused with the *nonlinear* power-law response of sensory systems over many decades of input magnitude, to which Stevens (*7*) has called attention. The difference is that in the linear power-law dynamics the noninteger exponent k applies to time (t^{-k}) and frequency (f^{k}), whereas in the nonlinear power-law behavior the k applies to the input itself (I^{k}). Some relationships between the two descriptions will, however, be developed.

Before proceeding to illustrate how nonuniformity over a cell can account for these power-law dynamics—using photoreception in the *Limulus* eye as an example—we describe briefly the recent studies which establish the "power-law dynamics problem."

Experimental Basis

Figure 1 shows the time dependence of the outputs of several receptor preparations. In each case, a small, maintained step increase in the stimulus has been imposed at time $t = 0$. After the initial fluctuations (not plotted here) associated with the high-frequency dynamics of the receptor have settled out, the response (discharge rate in impulses per second) drifts slowly back toward some maintained level. Curiously, this drift appears for a considerable time as an almost straight line when plotted, as in Fig. 1, on double-logarithmic coordinates. Because such a line can be represented by the equation

$$\log(\text{Response}) = \log C - k \log(t)$$

This article was prepared while Dr. Thorson was a research fellow, and Dr. Biederman-Thorson was a von Humboldt fellow, at the Max-Planck-Institut für Verhaltensphysiologie, 8131 Seewiesen, Germany. Dr. Thorson is now affiliated with the Department of Zoology, Oxford University, Oxford. The authors' address is The Old Marlborough Arms, Combe, Oxford, England.

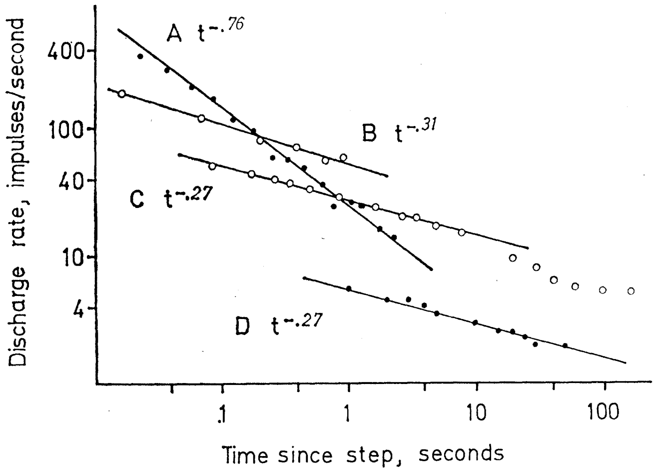

Fig. 1. Decay of "adaptation" of the nerve-impulse frequency in four kinds of receptor axons following a maintained step increase in the stimulus. The slopes of the straight lines indicate values of k in the function t^{-k}, to which the frequencies are nearly proportional over about two decades of time. *A*, Cockroach-leg mechanoreceptor (*8*), distortion of tactile spine on the femur; *B*, slit sensillum on the leg of the hunting spider (*71*), 1200-hz airborne sound; *C*, stretch receptor (slowly adapting) of the crayfish (*9*), 0.77-mm increase in stretch; *D*, single *Limulus* lateral-eye eccentric cell, increase of discharge rate above light-adapted level (*10*), 25 percent increase of light intensity. Similar adaptation is reported (*72*) in mammalian carotid-sinus baroreceptors, joint receptors, and atrial stretch receptors of the heart.

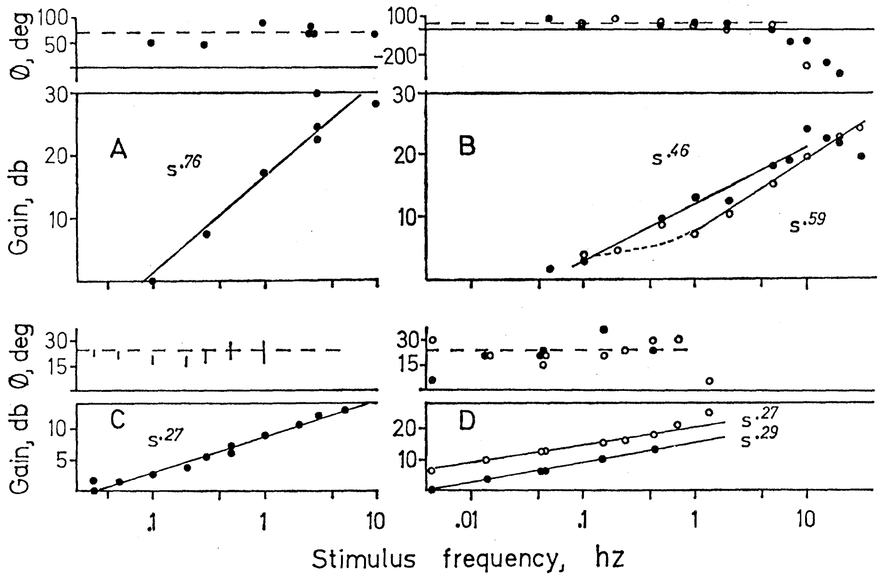

Fig. 2. Frequency responses of discharge rate in four kinds of single axons with small-signal, constant-amplitude sinusoidal driving of the stimulus. Gain at each frequency (in "power" decibels) is 20 $\log_{10}$(peak-to-peak response amplitude/arbitrary reference level). Phase (ϕ) is the phase lead of the nearly sinusoidal response with respect to the input waveform, so that negative values represent phase lags. Solid straight lines emphasize regions in which the shape of the gain data may be described approximately by the gain $(2\pi f)^k$ of the transfer function s^k, and dashed lines the corresponding phase lead ($k\pi/2$ radians) for s^k. *A, C,* and *D* represent companion experiments upon the receptors of *A, C,* and *D* in Fig. 1, and the values of k match. Companion data for the two different experiments labeled *B* in Figs. 1 and 2 are not available. *A*, Cockroach-leg mechanoreceptor (*8, 73*); *B*, averaged spike responses of "on" (solid circles) and "off" (open circles) ganglion cells of the cat retina under sinusoidal modulation of diffuse retinal illumination (*62*), replotted in decibels. At low frequencies, except for the small phase lead, the on-cell is nearly in phase, and the off-cell nearly 180° out of phase, with the modulating light; therefore the off-cell phases have been shifted 180° and plotted with those of the on-cell. The two slopes require phases of 42° and 53°; only one dashed line is shown, at 47°. *C*, Crayfish stretch receptor; vertical bars give range of phase uncertainty (*9*). *D*, single *Limulus* eccentric-cell response (*10*) to 20 percent modulation of illumination (solid circles, 610 lumen/m^2; open circles, 6 lumen/m^2; both in a spot of 100 μm diameter) to which the ommatidium had been adapted for about 30 minutes. The dashed-line phase requirement (24°) is that for the $k = 0.27$ slope. The extra points at 0.045 hz are from a repeat of that condition at the end of each frequency-response measurement series. The variations in frequency response of a locust optomotor response (not shown), with change of background intensity, are also represented closely over three decades of frequency by s^k (*11*).

where C and k are constants giving magnitude and slope, the response itself is decaying as

$$\text{Response} = Ct^{-k},\ t > 0$$

These power-law decays have been shown to be characteristic of the "small-signal" responses of many receptors; in such measurements, receptors are stimulated by small perturbations of their inputs within a range for which they are known to behave nearly linearly by a variety of tests (*8–11*). Therefore, despite the troublesome exponent, we are dealing with nearly linear dynamics: if the input is doubled, the response is doubled and the shape of the transient response waveform is unchanged.

A central notion in dynamic analysis is that it sometimes helps to consider the description of a system both in the time domain (as in Fig. 1) and in the frequency domain. Although the temporal response to a step increase of the input is often simpler to measure experimentally, the more cumbersome measurements of frequency response can provide noise rejection or a more sensitive guide to the behavior of a system over a restricted range of rates of change of the input. Moreover, for linear systems full knowledge of the frequency response (or transfer function) serves to define the step response, and vice versa.

The transfer function (*12*) of a linear transducer with step response t^{-k} is proportional to s^k, where s is the Laplace variable (*13*). The corresponding frequency response therefore (*14*) has gain which varies as f^k where f is frequency (a straight line of slope k if log gain is plotted against log frequency) and has a frequency-independent phase lead of $k \times 90°$ with respect to a constant-amplitude sinusoidal input. Figure 2 shows that both expectations are approximately realized over two or more decades of frequency for the receptors *A, C,* and *D* of Fig. 1 (Fig. 1B and Fig. 2B represent different receptors). Moreover, the values of k correspond.

Power-law dynamics are also implicit in another kind of experiment. In studies of movement perception, where a periodic pattern or other stimulus is moved past the eye with a range of velocities, receptors are stimulated at differing frequencies. Since the responses are "turning tendencies" or discharges of higher-order units, the

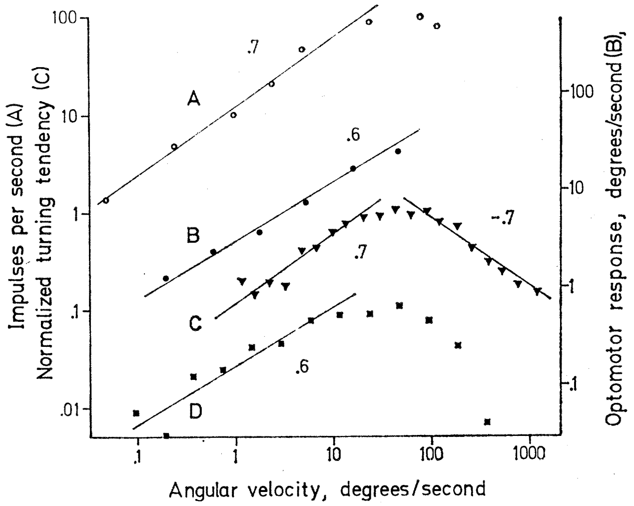

Fig. 3. The magic of the number 0.7 ± 0.1. Four experiments quantifying visual movement perception in which power-law dynamics of receptors or further neural processing (or of both) can be implied. *A*, Average discharge rate of a class-2 ganglion cell in the frog retina plotted against the angular velocity of an 0.7° black dot moved through its visual field (*74*); *B*, turning tendency of the fly *Eristalis* (compensatory angular velocity of a substrate held by the legs as a striped drum is rotated about the fixed animal) as a function of angular velocity of the surrounding striped drum (*75*); *C*, turning tendency (a linear function of the probability of turning in the direction of striped-drum rotation) of the weevil *Chlorophanus*, walking on a Y-maze globe, as a function of drum angular velocity (*76*), replotted logarithmically; *D*, averaged turning torques of six fixed, flying houseflies as a function of angular velocity of a striped drum (*77*), replotted logarithmically.

interpretation is less direct than in experiments with single cells (Fig. 2), but it is noteworthy that power-law relationships suggesting s^k-like behavior are often reported. In Fig. 3 we show a number of examples of this phenomenon.

Current Interpretations in Sensory Physiology

The fact that data on sensory adaptation are often of the form t^{-k} was first called to our attention by Chapman and Smith (*8*). They repeated Pringle and Wilson's (*15*) dynamic analysis of the cockroach-leg mechanoreceptor, found step responses such as those in Fig. 1, and showed that the frequency response included a corresponding s^k-like region (Fig. 2). Pringle and Wilson had originally described these step responses with a sum of three empirically chosen exponential decays. As we shall see below, if enough exponentials are used such a description can be as good as t^{-k}.

To our knowledge, just three specific mechanisms have been suggested as possible explanations of the s^k-like behavior of single receptors. Brown and Stein (*9*), finding that s^k (with k in the region 0.2 to 0.3) described approximately the dynamics of their crayfish stretch-receptor preparations, discussed the behavior of power-law spring (that is, one for which tension is a power function of length) connected to a viscous element. But as they pointed out, there are major difficulties in fitting this idea to their step-response data. Moreover, the small-signal sinusoidal response of fractional order is not available at all.

A second set of suggestions stems from a property of the diffusion (or "cable" or "heat") equation; that is, solutions for the Laplace transform of the variable treated involve the function $s^{0.5}$. For example, the current entering a suitable transmission line is just the half-order derivative (*13*) of time-varying input voltage. Reichardt and Varjú (*2*), pursuing the possibility that data from optomotor responses of weevils might require $s^{0.5}$ filters in the visual input channels, suggested that such a diffusional process could be responsible. More recently, Terzuolo and Knox (*16*), finding that lobster stretch receptors behave more according to $s^{0.5}$ than the $s^{0.25}$ that approximates the crayfish stretch-receptor responses in Fig. 2, pointed out that the dynamics relating intradendritic pressure to membrane potential (*17*) can involve a second-order nonlinear equation, and along with other factors account approximately for the data from lobster stretch receptors.

Still another approach is to ask, as Cole and Cole (*18*) did in 1941, whether a plausible Gaussian distribution about a single average rate constant might "flatten" or "smear" the curves expected from a simple first-order process sufficiently to account, within experimental error, for fractional-order dynamics. However, as Cole and Cole pointed out and as will become clear in our analysis, the distribution would have to be so broad that the attractive notion of variability about a single characteristic rate constant would tend to be lost. Other fractional-order analyses by the Coles and their colleagues (*19*) treat tissue and membrane impedance at very high frequencies.

None of the above suggestions suffices for two or more decades of, say, $s^{0.31}$ or $s^{0.76}$ at low frequencies as in Figs. 1 and 2. There may exist other, elementary physical processes that produce inherently such linear dynamics, but we have not been able to think of any.

Given this void, we suggested (*10*) that one might simply treat the power-law behavior as a weighted summation over a broad range of simpler exponential relaxation processes, as was discussed in the early literature of electrophysics and other fields. One can then ask whether there are physiological variables and relationships that correspond to such rules. We shall show that this procedure in fact generates testable hypotheses.

von Schweidler's Algorithm

The earliest example we have found of the distributed approach to power-law phenomena is in the early electrophysics literature (*20*) where t^{-k} decays were often reported for the discharge of charged Leyden jars. In an attempt to interpret such data, von Schweidler (*21*) pointed out in 1907 that by making use of the definition of the gamma function,

$$\Gamma(x) \equiv \int_0^\infty \lambda^{x-1} e^{-\lambda} d\lambda$$

one can write

$$t^{-k} = \frac{1}{\Gamma(k)} \int_0^\infty a^{k-1} e^{-at} da \qquad (1)$$

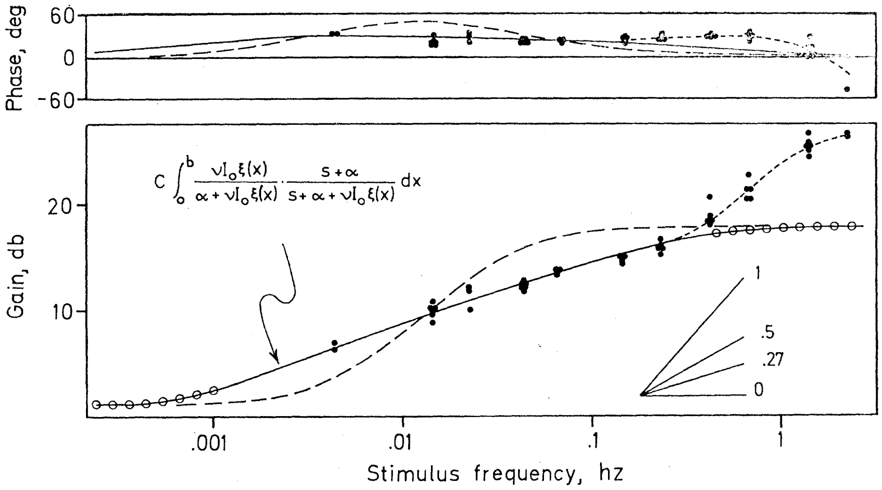

Fig. 4. A composite estimate of the small-signal dynamics, over four decades of low frequency, of the optically isolated *Limulus* eccentric-cell generator potential, when adapted for at least 30 minutes to an intensity of about 610 lumens/m^2 in a spot of 100 μm diameter. Solid circles represent data for rates of axon discharge from six isolated units (*10*), including the high-intensity data of experiment *D* of Fig. 2. The relation of the axon discharge to generator potential is treated in (*10*). The leveling off of the generator-potential frequency response (open circles at high frequency) at 1 hz in this range of intensity, as well as the direct transition to this level from an s^k-like region, are in accordance (*10*) with Pinter's (*34*) analysis of the generator-potential frequency response. The divergence (fine dashed lines) of axon-discharge gain and phase, above 0.2 hz, from that of the estimated generator-potential response corresponds quantitatively (*10*) to the known effects of "self-inhibitory" dynamics of the eccentric cell. Leveling off of the low-frequency response below 0.001 hz (open circles at low frequency) is derived from experimental estimates of the steady-state responses of the cells to changes of intensity. Estimates from long-term step responses (*10*) gave a steady-state response value 23 db below the response at 1.4 hz, whereas the slope of the steady-state data in Fig. 8 suggests a value as much as 29 db below. In this example we chose a level 25 db below the 1.4-hz gain—the choice affects principally the value of α in the analysis. The solid black lines represent gain and phase of the transfer function of Eq. 8 with parameters described in the text; the coarse dashed lines, those for the first-order "linear lead" network $(s + a_1)/(s + a_2)$ with center frequency at 0.013 hz and a total gain transition of 17 db.

In these equations, x is an arbitrary independent variable, λ is a variable of integration, and a is a rate constant. Thus the t^{-k} behavior can in principle arise from the summation of many different exponential decays (e^{-at}), each making a contribution which is proportional to its own rate constant a raised to the power $(k - 1)$. Since first-order kinetics—giving exponential decays—are common in nature, von Schweidler's equation should be a key to hypotheses about the events underlying power-law decays (*22*).

The transfer function of a device having a step response e^{-at} is that of the first-order high-pass filter, $s/(s + a)$; high-frequency signals are transmitted unaltered, but at frequencies below $a/2\pi$ transmission is proportional to frequency. Just as t^{-k} was decomposed into a linear combination of exponential decays with weighting function a^{k-1}, s^k can be represented as a sum over a continuum of high-pass filters with the same weighting function. That is,

$$s^k = \frac{1}{\Gamma(k)\Gamma(1-k)} \int_0^\infty a^{k-1} \frac{s}{s+a} da \qquad (2)$$

Equation 2 can be read directly as an algorithm for the synthesis of an s^k-like process. For example, to interpret the fractional-order dynamics of a sensory transducer, there are three things wanted. (i) There must be a first-order (that is, exponential) relaxation process, corresponding to $s/(s + a)$, which is rate-limiting (that is, its effect is manifest at the output) and which is quasilinear for small stimulus changes; the rate constant for this process is a. (ii) There must be many such processes, working simultaneously in the receptor in such a way that a is distinctly different for members of this ensemble. To account for two frequency decades of s^k, a must be distributed (or have a probability density) approximately as a^{k-1} over about two decades of variation of a. (iii) The outputs of all of these individual relaxation processes must be, approximately, summed in the output (for example, the generator potential) of the transducer. If these requirements are satisfied, the frequency response of the process will correspond to that of s^k.

Limulus Eccentric Cell

The nearly fractional-order dynamic response of the single uninhibited *Limulus* ommatidium (*10*) is illustrated in Figs. 2 and 4. It extends from about 0.2 hz down to the lowest frequency we have applied (0.004 hz) and probably to frequencies below 0.001 hz where the estimated steady-state response would be attained (*10*). At least two decades of $s^{0.27}$-like behavior are implied.

An eminently suitable relaxation process, which one can try in von Schweidler's algorithm, has already been suggested and shown plausible. Rushton (*23*) pointed out that the discrete potentials or "bumps" discovered by Yeandle (*24*) at low levels of illumination in the membrane potential of the *Limulus* eccentric cell, might underlie the "range compression" (*25*) or nearly logarithmic response of the eye to light. Since at low levels of illumination there appear to be rare large bumps and at higher levels frequent small bumps, it was tempting to ask whether bump size might be decreasing with increased light in just such a way as to produce the overall logarithmic response of the cell in the steady state. More recently, it has been shown that each bump is probably triggered by the absorption of a single photon (*26*), and that adaptation can occur locally—that is, to a different extent in different parts of the single receptor (*27–30*).

If bumps conforming to these rules were actually being summed to produce the generator potential, then one should be able to describe the generator potential in terms of the properties of a shot-noise process, with the shots representing bumps of a size and rate appropriate for the average intensity being applied. Dodge *et al.* (*31*) have shown that this view is compatible with the measured fluctuations of the generator potential.

As Adolph (*32*) and Dodge *et al.* (*33*) have pointed out, if bump size were determined by a balance between light intensity and some restoring process, then after a change in light intensity the bump size should take some time to "adapt" to a new equilibrium amplitude. Similarly, after a brief flash of bright light superimposed upon a steady background, bump size should be transiently depressed—in further agreement with their experimental results (*31*). The properties of such an "adapting bump" process are those of a high-pass filter; rapid changes of light are reflected in large changes in the output; but during slow changes the bumps have time to adapt so that less change in output occurs. Dodge *et al.* (*33*) represented this notion by fitting a first-order high-pass filter, with arbitrary rate constant, to their low-frequency data (which include only frequencies greater than 0.1 hz so that the s^k region is not apparent) in the same way that Pinter (*34*) described his *Limulus* generator-potential data at low frequencies (> 0.02 hz).

To apply von Schweidler's algorithm, we must formulate the adapting-bump idea more precisely. It seems clear that absorption of photons by rhodopsin, located in the micovilli of the retinula cells surrounding the eccentric-cell dendrite (*35*), leads to an increased conductance between the inside of the eccentric cell and a remote reference electrode (*36, 37*). Such an excitatory conductance change, with equilibrium potential near zero (*37*), can, of course account for the generator potential measured in the soma and for the spikes triggered in the axon.

It is not clear, however, just where or in what way this conductance change occurs. The measurements of Borsellino *et al.* (*38*) imply that there is at least as much change between retinula cell and remote tissue as there is between eccentric-cell dendrite and retinula cell. Moreover, if one photon is to induce a bump of several millivolts, amplification must occur. Adolph (*32*) has discussed this process in terms of the effect of a transmitter substance released by rhodopsin isomerization which acts on the relevant membranes as in a chemical synapse. Bass and Moore (*39*), on the other hand, have shown that if the membrane is electrically excitable, the opening of a single pore in the retinula-cell membrane by a photon capture might lead to sufficient active spread of depolarization to account for the conductance change (see also *40*).

Exponentially Restored, Poisson-Released Processes

Because we are concerned with the dynamics of local bump adaptation as they affect the next higher level of organization of the eccentric cell (that is, the generator potential), we shall consider here only the behavior of a broad class of such bump-producing mechanisms, defined as follows: (i) There is a large ensemble of sites in each region of the rhabdome (for example, two such sites are illustrated in the region labeled dx in Fig. 5). A site is defined operationally by the following considerations. Each site captures photons from the local instantaneous photon flux $I(t)$ according to an effective cross section v. (If there are m rhodopsin molecules serving a site, v/m is the net molecular cross section of rhodopsin for such captures.) (ii) Whenever a site, say the i^{th} one, captures a photon, it causes a transient conductance change of standard shape and of amplitude proportional to its normalized "capability" q_i at that instant, as illustrated in Fig. 5 for two such sites. This event reduces q_i to zero, following which it is restored by

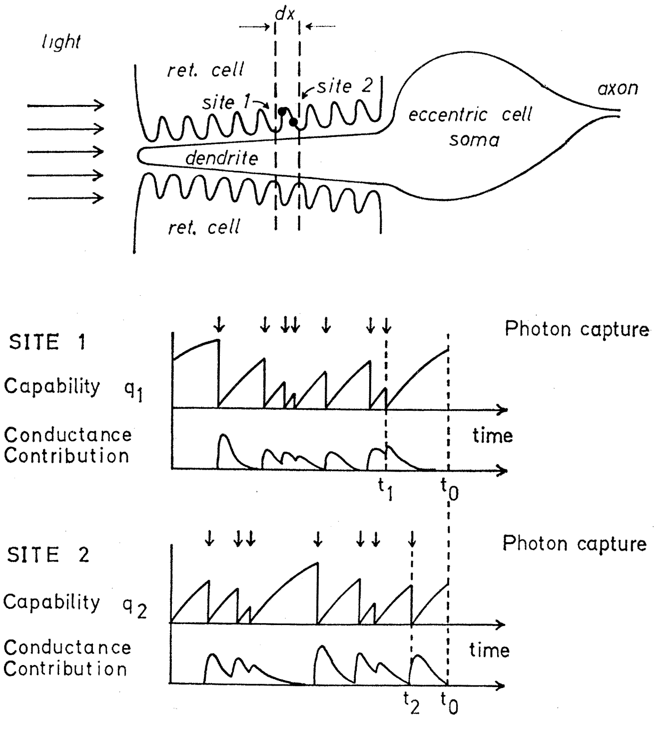

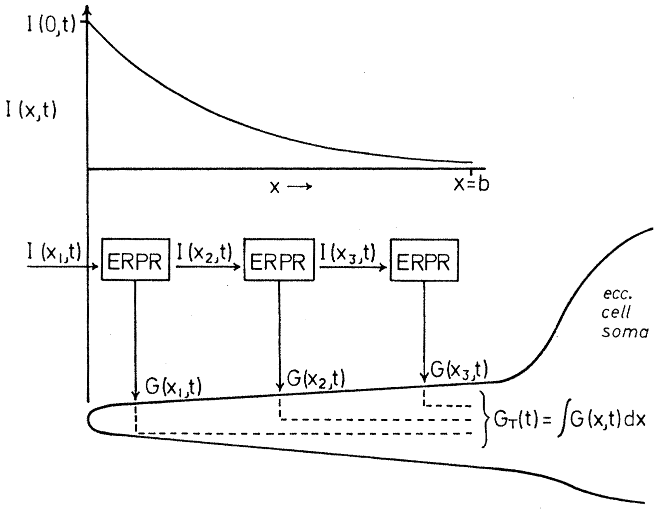

Fig. 5 (left). Schematic diagram of the *Limulus* eccentric-cell photoreceptor. The undulating borders of the retinula cells schematize the rhabdomal microvilli where the visual pigment rhodopsin resides. Two (solid circles) of the large number of transduction "sites" (see text) in each small region dx of the rhabdome are labeled sites 1 and 2 (dx is an elemental increment along the x (longitudinal) axis of the dendrite over which we integrate). Below, the exponentially restored, Poisson-released (ERPR) operation of the variable q for the two sites, and the corresponding "bumps" of conductance change are illustrated. The exponential recovery of q is probably somewhat slower, with respect to the time-scale of the bumps, than shown here; t_1 and t_2 for the two sites are the times of most recent photon capture, at observation time t_0, used to derive the light-intensity-to-conductance dynamics (*42*). Fig. 6 (right). "Distributed efficacy" formulation for the hypothetical case in which all receptor nonuniformity is treated as though spatial variation of photon flux sufficed for the distributed dynamics. The three x values illustrated represent the continuum actually treated. The problem is to find the function $I(x,t)$ [$= I(0,t)\xi(x)$] such that the total conductance change $G_T(t)$ agrees with estimates of the conductance dynamics of the cell. The rate constants of the local ERPR processes are functions of the local photon flux.

metabolic work at a rate proportional to its instantaneous state of depletion—so that q_i varies between 0 and 1 as

$$q_i(t_o,t_i) = 1 - e^{-\alpha(t_o - t_i)} \tag{3}$$

where t_o is the time of observation of the system, t_i is the time of the most recent photon capture by the i^{th} site, and α is a restoration rate constant.

In the case of a transmitter system, α would correspond to the rate constant for a process by which transmitter packets or vesicles are replenished following release; in the photoexcitation theory of Bass and Moore, α could represent the rate at which an ion pump or diffusion can restore the essential local ionic imbalances in the confined spaces about the microvilli. In either case, as shown in Fig. 5, it is clear that this set of rules, which, for a local ensemble of such sites within dx, we call an exponentially restored, Poisson-released (ERPR) process, produces large infrequent bumps in low photon fluxes and small frequent ones in high fluxes.

Now let us consider the dynamics of the ERPR process, for comparison with von Schweidler's algorithm. The problem is to find the time-varying conductance produced by summed action of the local ensemble (within dx) of n such sites, when all are subjected to a time-varying local photon flux $I(t)$.

We follow Dodge *et al.* (*31*) in treating the conductance underlying the generator potential as a shot-noise signal (each shot being one bump) whose amplitude has an expectation equal to a product of the rate, the effective amplitude, and the effective duration of such shots. Here, however, we assume for the moment a standard shape for all shots (*41*) so that it is only their amplitudes and rates that vary, in accordance with q and I, respectively. Moreover, the present process is nonstationary in time, and our averaging will be done over the large ensemble of sites in each dx in Fig. 5. We estimate the instantaneous expectation $G(t)$ of local conductance as proportional to the product of instantaneous local photon capture rate $\nu I(t)$ and the instantaneous expectation of local capability $\bar{q}(t)$, with all expectations taken over the local ensemble of n sites. That is,

$$G(t) = C_0 \nu I(t) \bar{q}(t) \tag{4}$$

where C_0 is a constant. This product may also be thought of as the instantaneous expected rate of release of a "transmitter," to which the transmitter concentration is about proportional, over a wide range, if the transmitter is very rapidly inactivated (that is, if the shots are brief) at a rate proportional to its concentration.

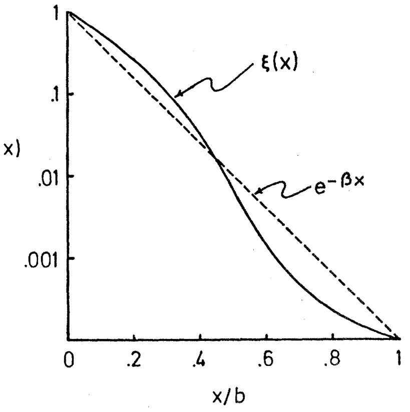

Fig. 7. The spatial efficacy function $\xi(x)$ which produces both the s^k-like small-signal dynamics of Fig. 4 and the nearly logarithmic steady-state response of Fig. 8, derived as described in the text. The function $e^{-\beta x}$ is included for comparison.

It remains for us to characterize $\bar{q}(t)$ for the local ensemble in a time-varying photon flux. It can be shown (*42*) that $\bar{q}(t)$ is conveniently treated in terms of its differential equation,

$$\frac{d\bar{q}(t)}{dt} = \alpha - [\alpha + \nu I(t)]q(t) \tag{5}$$

and one initial condition. For example, with $I(t) = I_0$ in the steady state, the value of $\bar{q}$ in the steady state is

$$\bar{q}_0 = \frac{\alpha}{\alpha + \nu I_0}$$

which can be taken as an initial condition in computing the response to subsequent changes of intensity.

Equation 5 shows that the rate of change of average bump height depends upon the local light intensity at each instant of time. For comparison with the data for the small-signal dynamics, however, we need the transfer function relating small fractional changes of intensity $i(t)$ to small fractional changes of conductance $g(t)$. Incorporating small signals about I, G, and $\bar{q}$ in Eqs. 4 and 5 and taking Laplace transforms, one finds, to first order in the small changes, that the local light-to-conductance transfer function of the ERPR process in each dx is

$$\frac{g(s)}{i(s)} = C\frac{s + \alpha}{s + \alpha + \nu I_0} \tag{6}$$

where C is a constant, independent of I_0 and s. This equation describes a first-order high-pass filter or "linear lead network" with a transition of gain from $C\alpha/(\alpha + \nu I_0)$, at frequencies less than $\alpha/2\pi$, to C at frequencies greater than $(\alpha + \nu I_0)/2\pi$. It specifies, quantitatively, the way in which small rapid changes of intensity produce larger changes of conductance than do small slow changes.

A Range of Rate Constants

The importance of Eq. 6, in terms of von Schweidler's algorithm, is that it defines, in the small-signal behavior of the ERPR process, a first-order relaxation having a rate constant ($\alpha + \nu I_0$, which can be considered analogous to a in Eqs. 1 and 2) that is dependent upon three specific physical quantities. These are the metabolic restoration rate α, the photon-capture cross section ν, and average local light intensity I_0, each applying in the small region dx of Fig. 5. If any or all of these take on different values in different parts of the rhabdome, we are in a position to ask whether von Schweidler's second requirement, a suitable range of rate constants, is fulfilled.

Although it is plausible that α and ν vary over the rhabdome, perhaps because of nonuniform mitochondrial density (*43*), and varying "site"-to-rhodopsin ratios, respectively, it is convenient to discuss the required nonuniformity in terms of the local light flux itself. A collimated photon flux entering a uniformly absorbing medium declines exponentially with depth of penetration. Absorption by rhodopsin alone, in the 100-micrometer depth of the *Limulus* rhabdome, ought not to reduce the entrant flux by more than about 15 percent (*35*). Effects of back and side scattering, absorption by structures other than rhodopsin, and refractive effects at the tip of the rhabdome will certainly cause greater nonuniformity. Local illumination can apparently vary by a factor of 100 over the photosensitive region of the retinal receptor of the squid eye (*28*, *29*). Although the extent of these effects is unknown in *Limulus*, Dodge *et al.* (*33*) comment that their failure to describe their low-frequency data with a first-order filter may imply nonuniform light absorption. Perhaps the most likely contributor to nonuniformity of light in the light-adapted state in

Limulus is the presence of pigment granules which migrate, in light adaptation, to surround the rhabdome (*44*) and can reduce internal reflection of light within it. For simplicity in this example, then, we will discuss the nonuniformity of the rate constants in terms of an equivalent spatial variation of local light intensity along the rhabdome, as shown schematically in Fig. 6. In general, however, we use the term "nonuniform efficacy" as a reminder that we could allow α and ν to vary as well, and that the method applies to distributed formulations other than that in the present shortage.

Summation of Conductance Changes

Finally, consider von Schweidler's third requirement. Here, it dictates that the conductance changes produced by all of the local ERPR processes (at different x's in Fig. 5) must be approximately summed in their combined effect upon generator potential and spike initiation.

This amounts to our treating the idealized eccentric-cell dendrite as having a very large length constant, so that the total conductance change as measured at the soma is nearly the sum of the local conductance changes per unit length as schematized in Fig. 6. The dendrite tapers from about 24 μm to 4 μm in its 100-μm length (*45*). Although the large size suggests the assumption of large length constant, the taper is of interest and could in principle be factored into our efficacy distribution once the stimulus-sensitive membranes in the ommatidium are identified with certainty. Moreover, for the low-frequency small-signal dynamics at a single average input intensity we can for the moment ignore the nonlinear transformation between conductance and generator potential, and proceed to compare our conductance calculation (for frequency-response shape) directly with the estimated generator-potential dynamics of Fig. 4.

If the conductance change per unit length is determined in each region dx by Eqs. 4 and 5, where G, I, and q are now written as functions of x as well as of t, then the total conductance change $G_T(t)$ of the idealized dendrite (of length b) is

$$G_T(t) = \int_0^b G(x,t)dx \qquad (7)$$

Introducing small fractional changes $g_T(t)$ of total conductance $G_T(t)$ and the small fractional changes $g(x,t)$ (from the time-domain analog of Eq. 6, written for each x) of local conductance per unit length $G(x,t)$, and taking Laplace transforms in Eq. 7, one finds that the small-signal transfer function relating input intensity changes to total conductance changes is

$$\frac{g_T(s)}{i(s)} = \frac{C \int_0^b G_0(x) \dfrac{s+\alpha}{s+\alpha+\nu I_0(x)} dx}{\int_0^b G_0(x)dx} \qquad (8)$$

where C is constant and $G_0(x)$ [also a function of $I_0(x)$] is the steady conductance per unit length defined by Eqs. 4 and 5. With this prediction of the small-signal dynamics, we are now in a position to see what efficacy distribution [here, $I_0(x)$] over the dendrite enables Eq. 8 to describe the data of Fig. 4.

Determination of the Distribution

To discuss the shape of a spatial intensity distribution $I_0(x)$ which would suffice for the *Limulus* frequency response, we define a dimensionless function $\xi(x)$, a spatial "efficacy" function, so that $I_0(x) = I_0\xi(x)$, where I_0 is the peak or entrant steady light flux [that is, $\xi(0) = 1$] upon which the small perturbations are imposed.

The formal similarity of Eq. 8 and Eq. 2, the frequency-domain equivalent of von Schweidler's equation, now permits straightforward calculation (*46*) of $\xi(x)$ such that the *Limulus*-eye generator-potential dynamics of Fig. 4 are accounted for. The correspondence requires that $k \doteq 0.27$, $\alpha \doteq 0.006$ sec^{-1}, $\nu I_0 \doteq 3$ sec^{-1}, and a choice of the ratio $\xi(0)/\xi(b)$ on the order of 10^3 or 10^4. The corresponding solution for $\xi(x)$ is shown (solid line) in Fig. 7. That this $\xi(x)$, used to determine $I_0(x)$ in Eq. 8, produces an excellent description of the generator-potential dynamics is shown in Fig. 4 (solid line). In order to emphasize the relative inadequacy of a single first-order "linear lead" network, invoked in other studies of the low-frequency dynamics, we include the gain and phase (coarse dashed lines) for such a process in Fig. 4.

Range Compression in the Steady State

From Rushton's original suggestion that the adapting bumps might underlie the Weber-Fechner or logarithmic behavior of the *Limulus* ommatidium, and from our specific formulation of one type of ERPR process (Fig. 5), one can intuit that such a process will map a wide range of input intensity onto a restricted range of output—that is, perform nonlinear range compression.

Thus far we have treated only the nearly linear response of the multiple-ERPR process to small perturbations about a steady level of input light intensity. Now, however, we shall consider the steady conductance changes produced by this nonlinear process as input intensity I_0 is varied over a wide range. The total steady-state conductance change in our formulation is

$$\bar{G}_T(I_0) = C_1 \int_0^b \frac{\nu I_0 \xi(x)}{\alpha + \nu I_0 \xi(x)} dx \qquad (9)$$

where C_1 is constant and the integrand represents the local conductances per unit length of Eqs. 4 and 5, which vary hyperbolically with local intensity $I_0\xi(x)$. First consider the case in which $\xi(x)$ is exponential; that is, $\xi(x) = e^{-\beta x}$. If β is large enough (that is, if the intensity $I_0\xi(b)$ reaching the proximal, most shielded—or least responsive—sites of the receptor is small with respect to α/ν for the entire range of input intensities I_0 considered), then the solution of Eq. 9 is

$$\bar{G}_T(I_0) \doteq C_2 \log\left(1 + \frac{\nu I_0}{\alpha}\right) \qquad (10)$$

where C_2 is a constant (*47*). This familiar function, plotted in Fig. 8 as the solid line, has been used empirically by Rushton and others (*48*) to characterize quantitatively the static range compression measured in *Limulus* and other photoreceptors. In this function $\bar{G}_T$ varies nearly linearly with I_0 at low intensities, and near $I_0 \doteq \alpha/\nu$ there is a transition to logarithmic transduction of higher intensities, which is of course the Weber-Fechner relationship.

The specific form of Eq. 10 demands special comment: Because one cannot take the logarithm of an "intensity" but only of a dimensionless number, some constant with the dimensions of (intensity)$^{-1}$ must appear before I_0 in Eq. 10. In the empirical formulas (*48*) this assumes the form $1/I_d$, where I_d

is called a "dark light," an "Eigengrau," or a threshold reflecting a particular signal-to-noise ratio. In our simple example of distributed phototransduction in *Limulus*, "I_d" arises physically as α/ν (with the units of intensity, cm^{-2} sec^{-1}), the ratio of the transduction restoration rate to the effective capture cross section of ERPR sites for photons.

The solution of Eq. 9 for the steady-state response obtained if one uses the actual $\xi(x)$, in Fig. 7, derived from the low-frequency response data of Fig. 4, is also shown in Fig. 8 (solid circles). It differs very little from the $\log(1 + \nu I_0/\alpha)$ behavior over five decades of intensity, and in fact saturates appropriately whereas Eq. 10 does not.

Experimental measurements of "steady-state" conductance as a function of light intensity for the *Limulus* eccentric cell, as well as of "steady-state" generator potential and discharge rate in the axon, are available (*31, 33, 36, 49*) and all of these show several decades of range compression. Such data could be fitted roughly to or compared in detail with the functions and parameters of Fig. 8, suitably converting (*33*) from conductance to generator potential where indicated.

We have three reasons for not making this comparison. First, all earlier experimental measurements of the "steady state" of which we are aware define "steady state" as the response obtained near the end of a 10- or 20-second flash of light, usually applied to the dark-adapted, excised eye. However, our small-signal dynamic analysis (Figs. 1, 2, and 4), on which the present formulation is based, was done with the eye in situ (*50*) and well-adapted to the intensity I_0—stable discharge rates (± 20 percent or better) were obtained for periods of 30 to 90 minutes. To try to relate these actual steady states to the 10- to 20-second flash response usually studied, we repeated the large-step flash experiment; after a tendency to plateau in the region of 5 to 10 seconds, discharge rates declined steadily in the period 10 to 100 seconds, toward the maintained steady state at frequencies one-half to one-third those of the plateau. We cannot rule out, therefore, the possibility that the response near 5 to 15 seconds following large steps may be influenced by the dynamic interplay of several nonlinear mechanisms of transient adaptation.

Second, Barlow and Kaplan (*51*) have recently shown that the 5- to 10-second response (which they termed "steady state") plotted against intensity of a 10-second flash is entirely different in excised eyes from that measured with the eye in situ. Third, as we have made clear (*46*), our predictions of the effects of large changes in I_0 may suffer from our neglect here of such effects as pigment migration and bleaching.

We do, however, have enough information to inquire whether a region of the response predicted in Fig. 8 is compatible with the intensity dependence of the steady-state firing rates of the cells for which the dynamics in Fig. 4 were measured. To establish the approximate position on the "range-compression curve" of these firing rates, two of these cells were adapted for at least 30 minutes to intensities 1 and 2 log units, respectively, below the standard intensity level for the measurements of frequency response in Fig. 4 (*10*). Since we have already fixed the values of νI_0 and α for the standard level in order to fit the frequency response in Fig. 4 (that is, $\nu I_0/\alpha = 3/0.006 = 500$), the calculated steady response in Fig. 8 at the dimensionless intensity $\nu I_0/\alpha = 500$ must correspond to the average firing rate (in this case, 12 impulses per second) for these cells at the standard intensity. With the two ordinates in Fig. 8 chosen in this way, the measured discharge rates (open triangles and circles) plotted against intensity conform approximately to the predicted variation (solid circles) of the steady conductance in this range. This test would not be highly sensitive to a bad theory, particularly if $\nu I_0/\alpha$ for Fig. 4 were to have fallen below 500. Higher values, though, would produce a mismatch of the slopes. We claim only compatibility of the dynamic response at $\nu I_0/\alpha = 500$ with the steady-state predictions in this region.

Because we have been forced to choose $\nu I_0 = 3$ sec^{-1} at the illumination level of the experiments in Fig. 4, knowledge of the photon flux I_0 would serve to fix ν. Our standard level of illumination (*10*) corresponded to a corneal flux on the order of 3×10^{14} photons (555 nm) cm^{-2} sec^{-1}. If this were taken as the entrant flux I_0 at the tip of the rhabdomere, the corresponding value of the effective absorption cross section of a "site" ν would be about 100 Å^2. Although there is room for considerable rationalization in either direction, this value has at least the distinction of lying between that for the projected geometrical area of the rhodopsin molecule (*52*) and that for the capture cross section implied by the molar extinction for rhodopsin (*53*).

Finally, the "backward calculation" used (*46*) to derive $\xi(x)$ from the dynamic response in Eq. 8 can be applied to Eq. 9 so that steady-state responses of receptors, whether they obey a power law, or are logarithmic, or even nearly hyperbolic, can be employed to derive corresponding candidate distributions of local efficacy. For example, it is easily shown that local hyperbolic transducers with response of the form $I/(I + M)$, if M is distributed and the local contributions are weighted as M^{k-1}, produce in the aggregate the power-law response I^k which Stevens (*7*) has discussed. Alternatively, if I were considered to be distributed—as in our present example—each measured response characteristic would define a corresponding efficacy function $\xi(x)$.

Plausibility, Testability, and Generality

We have shown that one can account for both s^k dynamics at one average intensity and nearly logarithmic statics over several decades of intensity with a single distributed efficacy function $\xi(x)$. As one can infer from Fig. 7, the flattening of the required $\xi(x)$ at high values of efficacy [as compared with an exponential $\xi(x)$] might be expected in a dioptric apparatus where focusing and maximum bleaching occur in the most sensitive or active region of the rhabdome; but such rationalizations are probably premature. Rather, the general features of $\xi(x)$ in Fig. 7 suggest that one might search in the *Limulus* eye and other receptors for sufficient equivalent nonuniformity of $I(x)$, ν, and α—or for nonuniformity of alternative distributed phenomena in the operation of the receptor.

The experiments of Hamdorf and his co-workers (*28, 29*) on local adaptation within single visual cells are of interest in this regard. Hamdorf's (*29*) demonstration of relatively uniform local sensitivity along the dipteran rhabdomere, as measured by the early peak response of the dark-adapted eye to flashes, particularly if extended to the small-signal sensitivity in various light-adapted states, could exclude the possibility that the effective values of ν and α are strongly nonuniform over the dipteran receptor. Moreover, comparison of these response characteristics under local and normal illumination could exclude nonuniformity of the effective photon flux by scattering, absorption, and refraction—although not necessarily nonuniformity resulting from "nodal effects" on the order of the wavelength of the light.

In a sense, the greater the efficacy range required to describe the distributed effects, the less plausible is the approach. It should be clear, however, that intensity has been used in this example to represent the nonuniformity due to all parameters; if ν and I were to covary (effective absorption being matched to the regions of highest intensity in the rhabdome), then variation by a factor of 32 in each of the two variables might suffice for the $\xi(b) = 0.001$ condition discussed above. If α or ν were assumed to vary we would, of course, formulate Eq. 8 somewhat differently to describe the fractional-order response.

We stress, however, that even without nonuniformity of ν, α, or I, there remain alternatives for which the distributed-efficacy methods apply directly. Hamdorf (*54*) has pointed out that one plausible contribution to range compression lies in spatial occlusion effects, whereby photon absorptions close together in both time and space in the rhodopsin array may produce less effect than similar events more remote from one another. This is in a sense a generalization of the "compartment" notion of Wald *et al.* (*55*) and is analogous to allowing our hypothetical "site-to-rhodopsin ratio" to become a critical variable—treating spatial occlusion rather than the temporal occlusion in local sites we have stressed here. The expected efficacy of any photon capture then depends upon its expected separation in space from other contemporary captures, so that the nonuniformity over which one integrates is the distribution of such spacings in a small interval of time. In the simplest, one-dimensional example, such spacings are distributed exponentially (the Poisson process is considered in space rather than in time), and the unknown function in Hamdorf's counterpart of Eq. 9 would become the local occlusion effect versus spacing of captures. The methods of solution developed here would then apply to the prediction of particular spatial occlusion functions that can account for given receptor responses versus light intensity. More generally, one would treat spatial and temporal occlusion together; the fact that both may involve distributed effects is made particularly clear by Hamdorf's suggestion.

The "antidromic illumination" and other novel optical techniques of Kirschfeld (*4*) and Franceschini (*5*), particularly their recent measurements in vivo of the statics and dynamics of migration of screening pigments in individual receptors of dipterans, underline a possible further dimension of the distributed approach. Pigment migration can be rapid enough to provide high-pass-filter effects analogous in principle to those in our adapting-bump example. Extending the analogy to our distributed formulation, one can search for spatial nonuniformity both of screening pigment and of the factors determining its rate of migration.

The Vertebrate Retina

Since the old photochemical explanations of adaptation were set aside (*56*), a remarkable fortress of psychophysical evidence (*57*) has accumulated, supporting the idea that the extensive visual adaptation that occurs with fixed pupil size, and before appreciable pigment is bleached, is not to be sought in the rods and cones—but rather in cells of higher order. Alpern *et al.* (*58*) have demonstrated that certain signals from rods and cones (those which interact somewhere in the visual system to produce metacontrast) indeed appear to show several decades of near-linearity in flash intensity.

Rushton (*59*) and Hodgkin (quoted in *59*) have shown how the complexity of light adaptation as usually measured can be given a unified description; it is assumed that rod signals are pooled in a segment of "transmission line" similar to that discussed by Fuortes and Hodgkin (*60*). The output of the line is fed back to increase the shunt conductance of the line. If rod signals representing the rate of photon capture enter the line and rod signals representing the fraction of rhodopsin bleached add to the output and hence also to the feedback, then the output of the line may behave like subjective brightness.

The critical factor producing range compression in the formal Fuortes-Hodgkin scheme is the feedback, which progressively shunts the signals, reducing the gain of the system as the output increases (*61*). The same effect enhances high-frequency response in their explanation (*60*) of *Limulus* eye. As Fuortes and Hodgkin point out, the

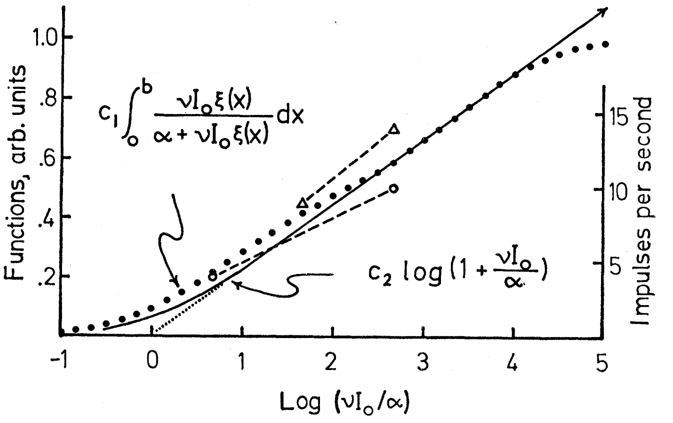

Fig. 8. Steady-state response (calculated conductance change) of the light-adapted *Limulus* eccentric cell (solid circles), predicted directly from the distributed formulation derived from the small-signal dynamics in Fig. 4. Pigment migration and bleaching are intentionally ignored in order to show that the "distributed adapting-bump" hypothesis can produce a range of nearly logarithmic behavior in the steady state. The function $\log(1 + \nu I_0/\alpha)$ (solid line), which the distributed model predicts if spatial efficacy is exponential, and its asymptote (fine dotted line) are shown for comparison. Open triangles and circles: steady-state firing rates (maintained ± 20 percent for at least 30 minutes) at different intensities for two (all available data) of the six cells with frequency response shown in Fig. 4. The high-intensity values are those for which the Fig. 4 frequency response was measured; since the dimensionless intensity $\nu I_0/\alpha$ from the fit in Fig. 4 is $(3/0.006) = 500$, the predicted response at $\nu I_0/\alpha = 500$ is matched to the average measured discharge rate at this level (12 impulses per second) by choice of the scale at the right. Axon discharge rate is expected to be linear in generator potential; the nonlinear transformation from conductance to generator potential has been neglected here since only a small range of moderate depolarization is implied by these discharge rates.

hypothetical variable fed back in *Limulus* apparently cannot be generator potential itself because changing this artificially does not alter the measured conductance.

The nonuniform-efficacy mechanism for range compression, which we have developed here, is distinct from the Fuortes-Hodgkin feedback scheme; one might, for example, hypothesize distributed inputs to Rushton's "pool" in such a way that von Schweidler's algorithm applies as in our *Limulus* example. A detailed formulation seems premature, but we note in its favor (i) that no hypothetical feedback is invoked, (ii) nonintegral-order dynamics are measured in cat ganglion cells (Fig. 2) (*62*), and (iii) that although we have treated quantitatively only the low-frequency and static behavior in our *Limulus* example, other inherent features of the distributed adapting-bump model make it an attractive alternative. These other features include enhanced high-frequency response with increased background intensity (*46*), and asymmetry (of Eqs. 4 and 5) in the proper sense—adaptation to light is much more rapid than that to dark.

In contrast to the above "nonreceptor" or "psychophysical" view of adaptation, Boynton and Whitten (*63*) find that the late receptor potential—thought to represent the signals to second-order cells—of retinal cones in the macaque monkey exhibits sufficient adaptation to account for a major portion of the human adaptation phenomena observed psychophysically in the same experimental apparatus. As they point out, the adaptation prior to bleaching can be understood to arise from the saturating power-law ($k \doteq 0.7$) response of the cones to light intensity. This amounts to range compression in the sense of our Fig. 8, and, as mentioned previously, a summation over local hyperbolic processes can produce such behavior in several ways. Each has heuristic physical implications; for example, if it were I that varied appreciably, then the overall bleaching kinetics could not be precisely hyperbolic but would be determined by an integral over the cell (*28*) similar to that for the response itself (*64*). Alternatively, the distribution of efficacy might apply over the several thousand cones which contribute to the late receptor potential measurement.

Boynton and Whitten also find that the late receptor potential shows a range of nearly linear response for stimuli superimposed upon a given background intensity (*63*). The adapting-bump formulation behaves in this way, at least for small stimuli which are brief with respect to bump adaptation rate. It is here especially clear that the dynamics can be critical, and that arguments based on steady-state considerations, when applied to such data (as well as to psychophysical data) in the absence both of hypotheses about the dynamics and of consideration of the durations of the various test flashes, can be at best preliminary.

Other Receptors

As a trial explanation of the fractional-order frequency response of crustacean slowly adapting stretch receptors (Figs. 1 and 2) (*9, 16*) consider for the moment that local strain produces local conductance changes (*65*) in the long dendrites [compare the shorter dendrites in the rapidly adapting stretch receptor (*66*)] aligned with the supporting muscle fibers. If these local processes adapt with strain-dependent rate constants, and strain is nonuniform along the dendrite [as is in fact the case for interfilament shear in the analogous distributed connections between an I filament with one free end and a strained A filament in insect muscle (*6*)], then one has a complete analogy with our *Limulus* hypothesis for the measured nonintegral-order dynamics. The idea can be tested with localized mechanical stimulation.

In chemoreception by insect antennal receptors, the dependence of the steady-state response upon stimulus concentration can be distinctly nonhyperbolic (*67*). Distributed effects analogous to those treated here, via nonuniform distributions of both odor substance (*68*) and pore channels (*69*) over the sensory surface have recently been identified, and offer testable bases for the characteristic responses of these receptors (*70*).

Summary

Dynamic description of most receptors, even in their near-linear ranges, has not led to understanding of the underlying physical events—in many instances because their curious transfer functions are not found in the usual repertoire of integral-order control-system analysis. We have described some methods, borrowed from other fields, which allow one to map any linear frequency response onto a putative weighting over an ensemble of simpler relaxation processes. One can then ask whether the resultant weighting of such processes suggests a corresponding plausible distribution of values for an appropriate physical variable within the sensory transducer.

To illustrate this approach, we have chosen the fractional-order low-frequency response of *Limulus* lateral-eye photoreceptors. We show first that the current "adapting-bump" hypothesis for the generator potential can be formulated in terms of local first-order relaxation processes in which local light flux, the cross section of rhodopsin for photon capture, and restoration rate of local conductance-changing capability play specific roles. A representative spatial distribution for one of these parameters, which just accounts for the low-frequency response of the receptor, is then derived and its relation to cellular properties and recent experiments is examined.

Finally, we show that for such a system, nonintegral-order dynamics are equivalent to nonhyperbolic statics, and that the efficacy distribution derived to account for the small-signal dynamics in fact predicts several decades of near-logarithmic response in the steady state.

Encouraged by the result that one plausible proposal can account approximately for both the low-frequency dynamics (the transfer function s^k) and the range-compressing statics (the Weber-Fechner relationship) measured in this photoreceptor, we have described some formally similar applications of these distributed effects to the vertebrate retina and to analogous properties of mechanoreceptors and chemoreceptors.

Conclusion

There are at least three reasons for considering further the role of distributed relaxation processes in sensory adaptation. First, one does measure both nonintegral-order dynamics and range compression in most receptors. Moreover, the nonuniformities of local "efficacy"—to which we have shown these characteristics can be related—must in fact occur to some extent. Finally, even if our several specific proposals should turn out to be experimentally excludable, these methods of treating distributed phenomena apply directly to alternative formulations and to other levels of the sensory transduction process. We hope that mathematical experiments, like those we have outlined here, will specify these relationships so that decisive physiological experiments can be done.

References and Notes

1. D. Lange, H. K. Hartline, F. Ratliff, in *The Functional Organization of the Compound Eye*, C. Bernhard, Ed. (Pergamon, Oxford, 1966), p. 425.
2. W. Reichardt and D. Varjú, *Z. Naturforsch.* **14b**, 674 (1959); D. Varjú and W. Reichardt, *ibid.* **22b**, 1343 (1967).
3. O. Trujillo-Cenóz and J. Melamed, *J. Ultrastruct. Res.* **16**, 395 (1966); V. Braitenberg, *Exp. Brain Res.* **3**, 271 (1967).
4. K. Kirschfeld, *Exp. Brain Res.* **3**, 248 (1967); in *Information Processing in the Visual Systems of Arthropods*, R. Wehner, Ed. (Springer-Verlag, New York, 1972), p. 61.
5. N. Franceschini, in *Information Processing in the Visual Systems of Arthropods*, R. Wehner, Ed. (Springer-Verlag, New York, 1972), p. 75.
6. J. Thorson and D. C. S. White, *Biophys. J.* **9**, 360 (1969); D. C. S. White and J. Thorson, *J. Gen. Physiol.* **60**, 307 (1972); *Prog. Biophys. Mol. Biol.* **27**, 173 (1973); A. F. Huxley and R. M. Simmons, *Cold Spring Harbor Symp. Quant. Biol.* **37**, 669 (1973).
7. S. S. Stevens, *Science* **170**, 1043 (1970).
8. K. M. Chapman and R. S. Smith, *Nature (Lond.)* **197**, 699 (1963). (Curve *A* in our Fig. 1 gives averages for sequential quintuples of the 80 data points following 0.015 second in Chapman and Smith's figure 2.)
9. M. C. Brown and R. B. Stein, *Kybernetik* **3**, 175 (1966).
10. M. Biederman-Thorson and J. Thorson, *J. Gen. Physiol.* **58**, 1 (1971).
11. J. Thorson, *Kybernetik* **3**, 53 (1966).
12. See, for example, B. M. Brown, *The Mathematical Theory of Linear Systems* (Wiley, New York, 1961).
13. Just as multiplication by s in the Laplace domain corresponds to first-order differentiation in the time domain, the operator s^k corresponds to the fractional-order differential operator. See, for examp→ J. D. Tamarkin, *Ann. Math. Ser. 2* **31**, 219 (1930); A. Erdelyi, Ed., *Bateman Manuscript Project, Tables of Integral Transforms* (McGraw-Hill, New York, 1954), vol. 1. The operation in the time domain is illustrated by its result on sin ωt: first-order differentiation yields $\omega \cos \omega t = \omega^k \sin(\omega t + k\pi/2)$, if $k = 1$. Fractional-order differentiation is definable by the latter expression if k is noninteger. s^k is a linear minimum-phase transfer function. To consider frequencies outside the range of data it represents in Fig. 2, one must amend it, for example, as $s^k/(s + b)$ to have a bound on high-frequency response, or as $(s + c)^k$ to introduce steady-state response c^k. (In these forms the inverse transformation is less tractable and one needs a computer to show that the step response can retain a large range of t^{-k} behavior.) As von Schweidler (*21*) put it, treating s^k (or t^{-k}) as though it applied for all s leads "to improbable consequences" [see, for example, A. Crowe, *Comp. Biochem. Physiol.* **20**, 13 (1967)]. Numerical methods for determination of transient response from arbitrary frequency-response data are discussed, for example, by A. Leonhard, in *Frequency Response*, R. O. Oldenburger, Ed. (Macmillan, New York, 1956). Where many decades of frequency (and hence of time) are involved, we have found it convenient to change variable from frequency to log(frequency) before evaluating the inversion integrals numerically.
14. Substitute $2\pi fj$ for s, where $j = \sqrt{-1}$, equate s^k to $re^{j\theta}$ and solve for gain r and phase θ.
15. J. W. S. Pringle and V. J. Wilson, *J. Exp. Biol.* **29**, 220 (1952).
16. C. A. Terzuolo and C. K. Knox, *Handbook of Sensory Physiology*, W. R. Loewenstein, Ed. (Springer, Berlin, 1971), vol. 1.
17. T. Teorell, *J. Gen. Physiol.* **42**, 847 (1959).
18. K. S. Cole and R. H. Cole, *J. Chem. Phys.* **9**, 341 (1941).
19. K. S. Cole and H. J. Curtiss, *Cold Spring Harbor Symp. Quant. Biol.* **4**, 73 (1936); R. H. Cole, *J. Cell. Comp. Physiol.* **66** (Suppl. 2), 13 (1965); K. S. Cole, *Membranes, Ions and Impulses* (Univ. California Press, Berkeley, 1968). The Coles and Schwann [H. P. Schwann, *Adv. Med. Biol. Phys.* **5**, 147 (1957)] have written excellent reviews of the very-high-frequency (kilohertz to megahertz) membrane-impedance work, in which "constant-phase-angle elements" and dielectric dispersion are inferred from the fractional-order effects measured.
20. R. Kohlrausch, *Poggendorfs Ann.* **91**, 56 and 179 (1854); W. Giese, *Ann. Phys. Chem.* **9**, 161 (1880); J. Curie, *Ann. Chim. Phys.* **18**, 203 (1889).
21. E. R. von Schweidler, *Ann. Phys.* **24**, 711 (1907). Apparently due to a misprint, von Schweidler's gamma function corresponding to the gamma function in our Eq. 1 contains an incorrect argument. The correct form is given in our Eq. 1. W. A. Yager [*Physics* **7**, 434 (1936)] refers to a possibly earlier analysis by Hopkinson (1876) but the citation seems to contain a misprint and we have not yet located it.
22. Since the composite decay (t^{-k}) and the rate constant distribution (a^{k-1}) in Eq. 1 are a Laplace pair, the algorithm generalizes conviently to any decay function and in this form is known in the polymer viscoelastic field as Alfrey's rule [see, for example, J. D. Ferry, *Viscoelastic Properties of Polymers* (Wiley, New York, 1961); A. V. Tobolsky, *Properties and Structure of Polymers* (Wiley, New York, 1960)]. Where the decay is not of a convenient functional form, Shimony [U. Shimony, *Proc. Inst. Elec. Electron. Eng.* **57.1**, 848 (1969)] describes numerical procedures for the generation of the rate-constant distribution.
23. W. A. H. Rushton, in *Light and Life*, W. D. McElroy and H. B. Glass, Eds. (Johns Hopkins Press, Baltimore, 1961), p. 706.
24. S. Yeandle, *Am. J. Ophthalmol.* **46**, 82 (1958).
25. A general term in sensory physiology for nonlinear transduction (logarithmic, or power-law, for example) in which the input variable has a larger range than the output variable seems useful. We have heard "range extension" (since the stimulus range is permitted to be large) and "response compression" (*63*) (since the output range can be usefully small). We choose "range compression" since this characterizes the process in terms of what the operation does mathematically.
26. M. G. F. Fuortes and S. Yeandle, *J. Gen. Physiol.* **47**, 443 (1964).
27. F. Ratliff, in *Functional Organization of the Compound Eye*, C. Bernhard, Ed. (Pergamon, Oxford, 1965), p. 187.
28. K. Hamdorf, J. Schwemer, U. Täuber, *Z. Vergl. Physiol.* **60**, 375 (1968).
29. K. Hamdorf, *Verh. Dtsch. Zool. Ges.* **64** (Jahresversamml.), 148 (1970).
30. In connection with the adapting-bump formulation miniature-potential size at synapses between Mauthner cells and giant fibers in the hatchetfish may also be reduced with high presynaptic frequencies [A. A. Auerback and M. V. L. Bennett, *J. Gen. Physiol.* **53**, 197 (1969)].
31. F. A. Dodge, Jr., B. W. Knight, J.-I. Toyoda, *Science* **160**, 88 (1968).
32. A. R. Adolph, *J. Gen. Physiol.* **48**, 297 (1964).
33. F. A. Dodge, Jr., B. W. Knight, J.-I. Toyoda, *How the Horseshoe Crab Eye Processes Optical Data* (IBM Research Publication No. RC 2248, 1968).
34. R. B. Pinter, *J. Gen. Physiol.* **49**, 565 (1966).
35. R. Hubbard and G. Wald, *Nature* **186**, 212 (1960).
36. M. G. F. Fuortes, *J. Physiol.* (*Lond.*) **148**, 14 (1959).
37. R. L. Purple and F. A. Dodge, *Cold Spring Harbor Symp. Quant. Biol.* **30**, 529 (1965). See also R. Millechia and A. Mauro, *J. Gen. Physiol.* **54**, 331 (1969).
38. A. Borsellino, M. G. F. Fuortes, T. G. Smith, *Cold Spring Harbor Symp. Quant. Biol.* **30**, 429 (1965).
39. L. Bass and W. J. Moore, *Biophys. J.* **10**, 1 (1970).
40. A. I. Borsellino and M. G. F. Fuortes, *Proc. Inst. Elec. Electron. Eng.* **56**, 1024 (1968); J. Y. Lettvin, W. F. Pickard, W. S. McCulloch, W. Pitts, *Nature* (*Lond.*) **202**, 1338 (1964).
41. In the spirit that too many nonlinearities spoil the intuition (concerning their individual effects), we leave out for the moment the inference of Dodge *et al.* (*31*) that bump duration may change somewhat over several decades of intensity, as well as Adolph's (*32*) bimodal distribution of bump height, which may be correlated with it.
42. First derive the probability density function f of the random variable $(t_0 - t_i)$ defined in Fig. 5 and Eq. 3, which is

$$f(t_o,t_i) = \nu I(t_i) \cdot \exp\left[-\int_{t_i}^{t_o} \nu I(\lambda)\, d\lambda\right]$$

where λ is an integration variable. This and Eq. 3 define the expectation $\bar{q}(t_o)$ of the random variable $q_i\ (t_o,t_i)$. Differentiating the expression for $\bar{q}(t_o)$ with respect to t_o, one is rewarded with the recurrence of the integral over all t_i, and Eq. 5 follows immediately. We thank Dr. Henry P. Kramer (Kramer Research, Inc., Santa Barbara, California) for his advice on the derivation.
43. O. Trujillo-Cenóz and J. Melamed, in *Functional Organization of the Compound Eye*, C. Bernhard, Ed. (Pergamon, Oxford, 1965), p. 339.
44. W. H. Miller, *Ann. N.Y. Acad. Sci.* **74**, 204 (1958).
45. W. H. Fahrenback, *Z. Zellforsch.* **87**, 278 (1968); *ibid.* **93**, 451 (1969).
46. Let $s + \alpha$ in Eq. 8 correspond to s in Eq. 2, change variable in Eq. 8 from x to $\nu I_o \xi(x)$, and equate $G_o(x)$ along with the resulting Jacobian to $[\nu I_o \xi(x)]^{k-1}$. The strict correspondence forces Eq. 8 to behave as $(s + \alpha)^k$ over a finite range of frequencies. The differential equation for $\xi(x)$ generated by the above procedure is then solved, and parameters chosen (see text) so that Eq. 8 fits the data of Fig. 4. In principle, one can now use the fixed $\xi(x)$ and simply alter I_o to predict the intensity dependence of the dynamics over a wide range. Here, of course, this means ignoring the effects of pigment migration and bleaching [Hamdorf *et al.* (*28*) have shown that in some invertebrate rhodopsin systems, the backward reaction of metarhodopsin to rhodopsin is sufficiently prominent that the usual bleaching considerations do not apply]. One does retain a range of the $s^{0.27}$ response over several decades of I_o in Eq. 8, as the data of Fig. 2 require, but increasing I_o increases the high-frequency response more than the measured amount, since no separate high-frequency attenuation has been included. The latter must be taken into account before comparison can be made with, for example, the Fuortes-Hodgkin dynamics (*60*).
47. When we showed this result to Dr. David Lange he remarked that he thought Dr. Bruce Knight had previously derived a similar relationship. In their model, though, Dodge *et al.* (*31, 33*) [see also B. W. Knight, J.-I. Toyoda, F. A. Dodge, Jr., *J. Gen. Physiol.* **56**, 421 (1970)] "boldly assume," as Rushton suggested, that average bump height somehow falls off with intensity so as to produce the logarithmic steady-state response. What we have demonstrated here is a specific way in which this state of affairs can come about. Glantz [see (*48*)] employs the bump hypothesis and a membrane nonlinearity to derive a hyperbolic relationship between light intensity and visual generator potential. This function fits approximately his data for the crayfish receptors, which apparently are sensitive to intensity change over a relatively small range. Glantz assumes neither an intensity-dependent bump height nor spatial nonuniformity in the receptor.
48. W. A. H. Rushton, *J. Physiol.* (*Lond.*) **148**, 29 (1959); *ibid.*, p. 36; R. M. Glantz, *Vision Res.* **8**, 1407 (1968).
49. M. G. F. Fuortes and G. F. Poggio, *J. Gen. Physiol.* **46**, 435 (1963).
50. Our chief concern about the condition of the receptors in this study (*10*) was that a blood vessel, associated with the optic nerve and coursing near the eye, was opened. Barlow and Kaplan (*51*) have now identified this vessel as a branch of the hepatic artery, whose rupture near the optic nerve apparently does not interfere with circulation at the eye.
51. R. B. Barlow, Jr., and E. Kaplan, *Science* **174**, 1027 (1971).
52. G. Wald, *Science* **119**, 887 (1954).
53. ——→ and P. K. Brown, *J. Gen. Physiol.* **37**, 189 (1953).
54. K. Hamdorf, personal communication.

55. G. Wald, P. K. Brown, P. H. Smith, *J. Gen. Physiol.* **38**, 623 (1955).
56. See, for example, W. A. H. Rushton, *J. Opt. Soc. Am.* **53**, 104 (1963).
57. Well summarized by J. E. Dowling, *Science* **155**, 273 (1967).
58. M. Alpern, W. A. H. Rushton, S. Torii, *J. Physiol. (Lond.)* **206**, 193 (1970); *ibid.*, p. 209; *ibid.* **207**, 449 (1970); *ibid.*, p. 463.

→ W. A. H. Rushton, *Proc. Roy. Soc. Lond. Ser. B* **162**, 20 (1965).

60. M. G. F. Fuortes and A. L. Hodgkin, *J. Physiol. (Lond.)* **172**, 239 (1964).
61. This scheme involving feedback or "automatic gain control" [R. M. Boynton, *J. Opt. Soc. Am.* **53**, 165 (1963)] should be distinguished carefully from Kaissling's (*67*) notion for long very thin dendrites in which it is the distributed conductance changes due to the conductance-increasing stimulus that shunt the currents produced by additional stimuli, so that range compression occurs.
62. G. W. Hughes and L. Maffei, *J. Neurophysiol.* **29**, 333 (1966); see also L. Maffei, L. Cervetto, A. Fiorentini, *ibid.* **33**, 276 (1970).
63. R. M. Boynton and D. N. Whitten, *Science* **170**, 1423 (1970).
64. For example, if $I(x) = I_0 e^{-\beta x}$ and the steady-state fraction of pigment bleached at each $I(x)$ is $I(x)/[I(x) + Q]$ with Q constant, then the integrated fraction bleached over the receptor (or receptors) is

$$\left[\ln\left(1+\frac{I_0}{Q}\right)-\ln\left(1+\frac{I_0 e^{-\beta b}}{Q}\right)\right]/\beta b$$

so that the fraction bleached is about proportional to the logarithm of $(1 + I_0/Q)$ over a range determined by the size of β. Note that if the threshold ΔI for a visual response were proportional to I_0, as in the Weber-Fechner relationship, the S-shaped curves for bleaching plotted against threshold upon which Dowling and Wald remark for the rat retina [see, for example, figure 4 in G. Wald, P. K. Brown, I. R. Gibbons, *J. Opt. Soc. Am.* **53**, 20 (1963)] would be approximated. Such a comparison raises at least as many questions as it answers, because the same relationship is found when vitamin-A deficiency is substituted for the bleaching and because Dowling's curve for bleaching plotted against background illumination for the rat eye (*57*) is steeper, rather than more gradual, than the function $I/(I + Q)$.

65. See, for example, W. R. Loewenstein, *Cold Spring Harbor Symp. Quant. Biol.* **30**, 29 (1965).
66. E. Florey and E. Florey, *J. Gen. Physiol.* **39**, 69 (1955).
67. K.-E. Kaissling, in *Handbook of Sensory Physiology*, L. M. Beidler, Ed. (Springer, Berlin, 1971), vol. 4, p. 351.
68. R. A. Steinbrecht and G. Kasang, *Wenner-Gren Center Symp. Ser. Olfaction Taste* **4**, 193 (1972).
69. R. A. Steinbrecht, personal communication.
70. K.-E. Kaissling and J. Thorson, in preparation.
71. F. Barth, *Z. Vergl. Physiol.* **55**, 407 (1967).
72. S. Landgren, *Acta Physiol. Scand.* **26**, 1 (1952); W. D. McCall and W. J. Williams, *Fed. Proc.* **30**, 709 (1971); K. Chapman and J. H. Pankhurst, in preparation.
73. K. M. Chapman, *Bol. Inst. Estud. Med. Biol. Mex.* **21**, 141 (1963).
74. D. Finkelstein and O.-J. Grüsser, *Science* **150**, 1050 (1965).
75. H. Mittelstaedt, *Verh. Dtsch. Zool. Ges. Wilhelmshaven Zool. Anz.* **16** (Suppl.), 150 (1952). The data of B in Fig. 3 (H. Mittelstaedt, unpublished data) average the responses of two animals.
76. B. Hassenstein, *Z. Natursforsch.* **14b**, 659 (1959).
77. W. E. Reichardt, *Cold Spring Harbor Symp. Quant. Biol.* **30**, 505 (1965).
78. Our interest in nonuniform photoexcitation in various materials was stimulated during a valued period of study (by J.T.) under Dr. Richard E. Halsted (deceased) at the General Electric Research Laboratory (Schenectady, N.Y.). We thank Drs. Kent Chapman, Fred Dodge, James T. Enright, Russell Fernald, Walter Heiligenberg, Karl-Ernst Kaissling, Kuno Kirschfeld, Henry P. Kramer, G. David Lange, R. W. Preisendorfer, Richard F. Reiss, and David C. S. White for critical discussions. We also thank Drs. Horst Mittelstaedt, John W. S. Pringle, and Theodore H. Bullock, in whose laboratories the analysis was developed, for their encouragement and hospitality. We gratefully acknowledge partial support from USAF Office of Scientific Research grants 67-1337, 67-1337A and EOAR 69-64.

Norway: Small Country Plans Civil Science and Technology

Experience suggests how cooperative applied science programs can be linked to national goals and needs.

James Brian Quinn and Robert Major

A 2½-year project to develop coordinated, long-range plans for a major portion of Norway's civil science and technology programs has recently been completed. This exercise, undertaken by the Royal Norwegian Council for Scientific and Industrial Research (NTNF), illustrates many of the problems and opportunities of such planning in a small country (Norway's population in 1970 was 3.9 million).

Norway's situation regarding science and technology is similar to that of many other countries. Norway has limited scientific and technical manpower resources—some 9000 degree-holders primarily engaged in research and development (R & D)—yet it must compete in its major export markets with large, technologically advanced countries. Norway's industrial structure contains few large companies, but many small ones. Consequently, government and private industry must cooperatively support R&D in many fields. Even so, Norway must, of necessity, import most of its scientific and technological knowledge. Since its natural resources are already being extensively exploited—except for recently discovered hydrocarbons in the North Sea—Norway must depend on knowledge industries for future economic growth. Like many other countries, Norway faces the modern challenges of continued economic growth, maintenance of a good quality of life in its cities, and enlightened development of its extensive rural areas. Sophisticated application of science and technology will be necessary to attack these problems. Norway's approaches and experiences could be of interest to many.

Structure of Norwegian Science and Technology

Total expenditures for R & D in Norway were about 1100 million kroner in 1971, or approximately 1.2 percent of the gross national product. Table 1 shows how expenditures for R & D in Norway are distributed among sources of funds and performing institutions.

To stimulate and coordinate R & D in nonmilitary fields, there are three research councils: the Norwegian Council for Science and the Humanities, the Norwegian Agricultural Research Council, and the NTNF. Their activities cover virtually all subject areas except defense. The councils advise the ministries concerned with their respective fields, supervise certain research institutes, finance research projects and research capital needs, provide scholarships, and advise on education, training, and recruitment of scientific and technical personnel (*1*).

Dr. Quinn is Nathaniel Leverone professor of management, Dartmouth College, Hanover, New Hampshire 03755, and a consultant on long-range planning. Mr. Major is director of the Royal Norwegian Council for Scientific and Industrial Research, Box 279, Blindern Oslo 3, Norway.